

# Fisher Identifiability Analysis of Longitudinal Vehicle Dynamics: Theory and Experiments

Aaron Kandel<sup>a</sup>, Mohamed Wahba<sup>b</sup>, and Hosam K. Fathy<sup>c</sup>

<sup>a</sup> Department of Mechanical Engineering, University of California, Berkeley, Berkeley, CA 94704;

<sup>b</sup> Department of Mechanical Engineering, The Pennsylvania State University, University Park, PA 16802;

<sup>c</sup> Department of Mechanical Engineering, University of Maryland, College Park, MD 20742

## ARTICLE HISTORY

Compiled June 23, 2022

## ABSTRACT

This paper examines the impact of mean-square terrain variability on longitudinal chassis parameter identifiability. This analysis is motivated by the immediate value of effective parameter estimation in various applications, including chassis model validation and active safety. Relevant literature addresses this demand through algorithms capable of estimating chassis parameters for diverse computational and on-road conditions. While the limitations of such algorithms' accuracy with respect to some driving conditions have been studied, their dependence on road grade variability remains largely unexplored. We address this open question by presenting two key contributions. First, this paper presents analytic derivations of the Fisher information matrix associated with estimating mass, drag, and rolling resistance parameters from longitudinal dynamics. We validate the analytic sensitivity expressions using simulations and experimental data gathered from an instrumented Volvo VNL300 heavy-duty freight truck. Then, this paper presents Monte Carlo simulations which illustrate the average improvements in chassis parameter identifiability associated with drive-cycles characterized by higher mean-square road grade. Our simulation studies demonstrate this result under a variety of drive cycles.

## KEYWORDS

identifiability, parameter estimation, longitudinal vehicle dynamics, Fisher information

## 1. Introduction

This paper explores the impact of terrain variability on the identifiability of longitudinal vehicle chassis parameters. From a conventional engineering perspective, vehicle chassis parameter estimation is an important exercise for identifying and simulating the performance of relevant vehicle models. Industry has and will continue to value methods for evaluating vehicle performance subject to varied operating conditions and disturbances, given the value such studies provide as effective design tools. The historic strength, diversity, and impact of the literature on vehicle chassis parameter estimation is as a result unsurprising. This longstanding literature continues to be relevant to modern and developing vehicle technologies. For example, online mass estimation

has significant importance to active vehicle safety systems, which is reflected by recent regulations which mandate its inclusion in new vehicles [1]. Similarly, drag estimation can provide utility in quantifying the benefits associated with a heavy-duty vehicle's participation in a vehicle platoon [2]. Furthermore, as connected and automated vehicle systems are studied in greater detail, online parameter estimation algorithms will become increasingly important, as the function of connected and automated vehicle (CAV) system optimization will likely depend on accurate knowledge of parameters including vehicle mass, drag, and rolling resistance coefficients. This consideration becomes even more important when considering vehicles with highly variable loads. Principally among these includes freight trucks, which coincidentally are becoming a popular early application for research into CAV system optimization [3,4].

These technologies all share a strong dependence on the effectiveness and accuracy of both the vehicle model and estimation algorithm in use in their respective designs. Fortunately, the literature presents numerous parameter estimation algorithms which each possess relevant strengths under a diverse host of experimental conditions. Online mass estimation from vehicle dynamics is a frequent and diverse application of such research. An early example of this application is presented by Bae et al., where they apply a recursive least-squares algorithm (RLS) to obtain online estimates of longitudinal parameters including vehicle mass from experimental data [5]. Work by Fathy et al. has further explored the application of online mass estimation with judicious selection of vehicle dynamics with a fuzzy supervisor, which identifies predominantly longitudinal vehicle motion [6]. Vahidi et al. effectively estimate both vehicle mass and road grade through RLS utilizing multiple of forgetting factors [7]. Rhode et al. evaluate a generalized version of total RLS based on its experimental performance estimating longitudinal parameters including rolling resistance coefficients and vehicle mass with a longitudinal vehicle dynamics model [8]. The authors of this paper also explore offline nonlinear least-squares longitudinal chassis parameter estimation within the context of quantifying the impact of terrain variability on the identifiability of such parameters [9].

Vehicle chassis parameter estimation is by no means, however, limited to the use of longitudinal vehicle dynamics. For example, Rajamani et al. find that relevant suspension dynamics can be utilized to effectively estimate vehicle chassis parameters including vehicle mass [10]. Pence, Fathy, and Stein demonstrate that even with inexpensive instrumentation, vehicle mass can be effectively estimated from base excitation suspension dynamics [11]. Reina et al. utilize lateral vehicle dynamics with model-based estimation and extended Kalman filtering to estimate vehicle states and mass [12].

For such varied conditions, exploring factors which directly affect parameter identifiability can reveal fundamental and, in some cases, critically relevant limitations related to the design of the underlying problem. This question dates back to a landmark paper by Bellman and Astrom [13]. Examining limitations related to the identifiability of model parameters provides a uniquely rewarding opportunity to observe new insights related to the nature of such estimation problems. Such insights can allow us to address fundamental questions like "What conditions of an on-road experiment impose the biggest limitations on chassis parameter estimation accuracy?", or "In what ways does the evolution of the drive cycle affect the identifiability of vehicle chassis parameters?" We can also attempt to quantify the impact of the effects which are present in the scenarios posed by such questions, including for example quantifying the impact of terrain variability on vehicle chassis parameter identifiability. This is where a great deal of this paper's motivation lies.

Relevant literature has a longstanding footprint of work that recognizes the impact

of the design of a vehicle experiment on the accuracy of the resulting chassis parameter estimates obtained from that experiment's data. The SAE testing standard for longitudinal vehicle chassis parameter estimation outlines several basic experimental conditions which facilitate estimation accuracy [14]. Within another context, work by Muller et al. demonstrates that the addition of speed bumps to a road test allows relevant suspension parameters to be estimated with greater precision [15]. While such work effectively discusses some limitations of vehicle chassis parameter identifiability, there are still many relevant questions which remain unanswered. Our analysis of the literature shows that an understanding of the impact of terrain variability on longitudinal chassis parameter identifiability is largely unexplored. The objective of this paper is to build upon the exploratory nature of our past work in [9] by addressing this open question in greater detail.

The Fisher information metric is an effective means for quantifying local parameter identifiability within this context. Fisher information provides insight into the information a dataset contains about some set of relevant model parameters [17]. This metric can be used to quantify the degree to which estimates of model parameters are unique and accurate. Furthermore, the invertibility of the Fisher information matrix indicates whether the experiment in question can possibly yield uniquely identifiable parameter estimates. Specifically, the Cramér-Rao theorem states that the best parameter estimation covariance achievable by an unbiased estimator is given by the inverse of the matrix-formulation of Fisher information. The preliminary sections of this paper are focused on deriving analytic expressions for the Fisher information matrix for a longitudinal vehicle dynamics model with respect to vehicle mass, drag coefficient, and rolling resistance parameters. We achieve this by deriving analytic expressions for the sensitivities of the output velocity of the longitudinal model with respect to perturbations in each relevant chassis parameter and augmenting these sensitivities into the conventional formulation of the Fisher information matrix. After validating these results with those obtained from conventional numeric approximations of Fisher information, we conduct several Monte Carlo simulation studies based on varying driving conditions. This paper's results show that drive cycles characterized by a high degree of terrain variability will on average yield more accurate longitudinal chassis parameter estimates. While this paper's simulations are run with parameter values corresponding to those of heavy-duty vehicles, the results of these simulations are largely applicable to vehicles of varying types and sizes.

The remaining organization of this paper is as follows. Section II details our formulation of the longitudinal vehicle dynamics. Section III describes the format of the Fisher information metric corresponding to the longitudinal dynamics, based on the sensitivity of the vehicle velocity output with respect to perturbations in each vehicle chassis parameter (vehicle mass, drag coefficient, and rolling resistance coefficient). We describe our methods for obtaining analytic expressions for these sensitivities in Section IV, while including validation of our derivations through simulation and on-road experiments. Section V of this paper presents a series of simulation studies which reveal the relationships between terrain variability and chassis parameter identifiability for a range of driving conditions. Finally, after section V our conclusion summarizes and synthesizes insights from our principal findings.

**Table 1.** Longitudinal Dynamics Model

Value	Description	Units
$x$	position	m
$v$	velocity	$\frac{m}{s}$
$\dot{v}$	acceleration	$\frac{m}{s^2}$
$F$	wheel force	N
$\beta$	road grade	radians
$m$	vehicle mass	kg
$C_d$	drag coefficient	-
$\mu$	rolling resistance coefficient	-
$A_{ref}$	frontal area	$m^2$
$\rho$	air density	$[\frac{kg}{m^3}]$
$g$	gravitational constant	$\frac{m}{s^2}$

## 2. Longitudinal Vehicle Dynamics Model

The foundation of this paper's analysis utilizes a nonlinear longitudinal vehicle dynamics model adopted from the literature [12]. This model formulation allows us to evaluate the identifiability of vehicle mass, drag coefficient, and rolling resistance coefficient parameters under a range of on-road operating conditions and drive cycles. The full nonlinear state-space form is given by (1-2).

$$\dot{x} = v \quad (1)$$

$$\dot{v} = \frac{1}{m} [F - \frac{1}{2} \rho C_d A_{ref} v^2] - \mu g \cos(\beta) - g \sin(\beta) \quad (2)$$

where  $x$  is the vehicle's position,  $v$  is the vehicle velocity,  $\dot{v}$  is the vehicle acceleration,  $F$  is the propulsion force, and  $\beta$  is the road grade. Table 1 describes the relevant state variables and parameters of this model.

## 3. Formulation of Fisher Information

Fisher information is a metric which quantifies how much information a data set contains about a set of relevant model parameters [17]. Historically, the application of Fisher analysis to estimate variances of vehicle model parameter estimates is common and has demonstrated effectiveness in quantifying parameter identifiability for longitudinal vehicle dynamics. In a purely statistical context, the estimation variances for relevant parameters would normally be obtained by conducting an experiment numerous times and comparing parameter estimates obtained from each experiment. The impracticality of such methods for potentially online on-road experiments, however, necessitates the application of a Fisher information analysis to approximate relevant parameter estimation variances.

In formulating our Fisher analysis, we first define relevant system output and longitudinal chassis parameters from the model described by (1-2). We specifically select vehicle mass  $m$ ,  $C_d$ , and  $\mu$  to be the chassis parameters which we assume are being estimated:

$$\theta = \begin{pmatrix} m \\ C_d \\ \mu \end{pmatrix} \quad (3)$$

A Fisher information analysis must be done with selection of a measured output variable. In this paper, we use longitudinal vehicle velocity as our measured output, as this aligns with our experimental setup. We recognize that other variables (i.e. acceleration) could be used for such an analysis, but for the purpose of brevity we focus on a single measured output variable.

The Fisher information matrix quantifies an expected curvature (i.e. Hessian) of the likelihood function specifically around the parameter estimate  $\theta$ . Several assumptions based on the characteristics of a maximum likelihood estimator (MLE) can be leveraged to approximate the Fisher information matrix by  $H \approx J^T J$ , where  $J$  is the Jacobian [18]. This procedure yields a local approximation of the Fisher information matrix for a nonlinear dynamical model using output sensitivities as follows:

$$I(\theta) = \frac{S^T S}{\sigma^2} \quad (4)$$

where  $\sigma$  is the sensor error associated with output measurement noise for an assumed white, independent and identically distributed noise process. We note that

$$S_{ij} = \frac{\partial y(t_i)}{\partial \theta_j} \quad (5)$$

where  $i$  indicates the timestep and  $j$  indicates the parameter, is the sensitivity of the output with respect to each of the parameters.

Given our choice of output and parameters, the Fisher information matrix for our longitudinal vehicle dynamics model takes the following form:

$$I(\theta) = \frac{1}{\sigma^2} \begin{bmatrix} \sum_{i=1}^N S_{i;m}^2 & \sum_{i=1}^N S_{i;m} S_{i;C_d} & \sum_{i=1}^N S_{i;m} S_{i;\mu} \\ \sum_{i=1}^N S_{i;C_d} S_{i;m} & \sum_{i=1}^N S_{i;C_d}^2 & \sum_{i=1}^N S_{i;C_d} S_{i;\mu} \\ \sum_{i=1}^N S_{i;\mu} S_{i;m} & \sum_{i=1}^N S_{i;\mu} S_{i;C_d} & \sum_{i=1}^N S_{i;\mu}^2 \end{bmatrix} \quad (6)$$

where  $\sigma = 1 \frac{m}{s}$  and the output is velocity  $v$ .

Conventionally, (5) is approximated numerically via finite difference:

$$\frac{\partial v(t_i)}{\partial \theta_j} = \frac{v(t_i, \theta_j + \epsilon_j) - v(t_i, \theta_j)}{\epsilon_j} \quad (7)$$

Both output trajectories  $v(t_i, \theta_j + \epsilon_j)$  and  $v(t_i, \theta_j)$  are obtained from simulations using either known, or estimated parameter values.

In section IV of this paper, we derive analytic continuous-time expressions for the output sensitivities given by (5). We therefore must approximate the summations in the Fisher information matrix with integrals when using these analytic expressions:

$$I(\theta) = \frac{f}{\sigma^2} \begin{bmatrix} \int_0^T S_m(t)^2 dt & \int_0^T S_m(t) S_{C_d}(t) dt & \int_0^T S_m(t) S_\mu(t) dt \\ \int_0^T S_{C_d}(t) S_m(t) dt & \int_0^T S_{C_d}(t)^2 dt & \int_0^T S_{C_d}(t) S_\mu(t) dt \\ \int_0^T S_\mu(t) S_m(t) dt & \int_0^T S_\mu(t) S_{C_d}(t) dt & \int_0^T S_\mu(t)^2 dt \end{bmatrix} \quad (8)$$

where  $T$  is the final time and  $f$  is the sampling frequency.

If the Fisher information matrix is positive definite, the model parameters are said to be uniquely locally identifiable. Furthermore, the Cramér-Rao theorem states that

the best achievable estimation covariance is obtained from the inverse of the Fisher information matrix. The diagonal terms of this covariance matrix are the Cramér-Rao lower bounds of the estimation variances for each parameter estimate in  $\theta$ . These estimation error variances quantify the accuracy of the estimator. This paper's simulated and experimental identifiability analyses compare the error bounds obtained from Fisher analyses using both numeric and analytic methods.

## 4. Analytic Sensitivity Derivations

As described in Section III, our format of Fisher information utilizes expressions for the sensitivity of vehicle velocity with respect to perturbations in vehicle mass, drag coefficient, and rolling resistance coefficient parameters. In this section, analytic expressions for the sensitivity of vehicle velocity with respect to perturbation in vehicle mass,  $C_d$ , and  $\mu$  parameters are derived.

Subsection 4.1 details our derivation of the nominal longitudinal velocity trajectory, and subsection 4.2 describes our analytic derivations for the sensitivity expressions. Subsection 4.3 demonstrates the accuracy of our analytic expressions through relevant simulation and experimentation.

### 4.1. Obtaining the Nominal Velocity Trajectory

To obtain the nominal velocity trajectory for use in our sensitivity derivations, we start with the full nonlinear longitudinal dynamics model with generalized, time-varying propulsion force and road grade:

$$\dot{v}(t) = \frac{1}{m} [F(t) - \frac{1}{2} \rho C_d A_{ref} (v(t))^2] - \mu g \cos(\beta(t)) - g \sin(\beta(t)) \quad (9)$$

In this paper, we treat propulsion force and road grade as time varying parameters. In reality, they both depend on position which itself depends on time. We approximate them as time varying to simplify our derivations.

Writing (9) for a drive cycle subject to a flat terrain profile and constant propulsion force yields the following equation:

$$\dot{v}_0 = \frac{1}{m} [F_0 - \frac{1}{2} \rho C_d A_{ref} v_0^2] \quad (10)$$

Here, we take a flat terrain profile as the operating point for a linearization of the model. If we take the following perturbations:

$$F(t) = F_0 + \delta F(t) \quad (11)$$

$$\beta(t) = \beta_0 + \delta \beta(t) \quad (12)$$

with  $\beta_0 = 0$  and  $F_0$  being the force required for our vehicle to maintain a constant predetermined speed  $v_0$  across a flat terrain. We decompose these signals such that proper terms conveniently cancel once we plug them back into the linearized model. Next, we can subtract (10) from the expression we get by plugging in (11) and (12)

into (9) to obtain the following equation for  $\delta\dot{v}_n = \dot{v}_n - \dot{v}_0$ :

$$\delta\dot{v}_n = \frac{\delta F(t)}{m} - \frac{1}{m}\rho C_d A_{ref} (v_n^2 - v_0^2) + \mu g (\cos(\delta\beta(t)) - 1) - g \sin(\delta\beta(t)) \quad (13)$$

Furthermore, the term  $v^2 - v_0^2$  can be linearized into  $2v_0\delta v$  when neglecting higher order terms, where  $v_0$  is the constant speed obtained by applying the constant propulsion force  $F_0$  to the vehicle subject to a flat terrain:

$$\delta\dot{v}_n = \frac{\delta F(t)}{m} - \frac{1}{m}\rho C_d A_{ref} v_0 \delta v_n + \mu g (\cos(\delta\beta(t)) - 1) - g \sin(\delta\beta(t)) \quad (14)$$

Solving this ordinary differential equation with zero initial conditions for  $\delta v_n(t)$  yields the expression for perturbed vehicle velocity relative to steady state, with respect to an arbitrary time-varying terrain profile and propulsion force:

$$\delta v_n(t) = e^{-\frac{C_d A_{ref} \rho v_0 t}{m}} \int_0^t \sigma(\tau) \left[ \frac{\delta F(\tau)}{m} - g(\sin(\delta\beta(\tau)) - \mu + \mu \cos(\delta\beta(\tau))) \right] d\tau \quad (15)$$

$$\sigma(t) = e^{\frac{C_d A_{ref} \rho v_0 t}{m}} \quad (16)$$

We can add this expression to  $v_0$  to obtain the nominal linearized velocity trajectory for arbitrary time-varying terrain and propulsion force. This overall expression is essential to the analytic derivation of the sensitivity of velocity with respect to perturbations in each chassis parameter  $m$ ,  $C_d$ , and  $\mu$ .

## 4.2. Sensitivity Derivations

The following subsections detail analytic calculations for the sensitivities of velocity with respect to perturbations in each longitudinal chassis parameter  $m$ ,  $C_d$ , and  $\mu$ .

### 4.2.1. Sensitivity of Velocity with Respect to Vehicle Mass

To find an equation describing the sensitivity of vehicle velocity with respect to perturbations in vehicle mass  $m$  we conduct the following analysis. Our first step is to rewrite the full longitudinal model with a percent perturbation applied to instances of the mass parameter.

$$\dot{v} = \frac{1}{m(1 + \epsilon_m)} \left[ F(t) - \frac{1}{2}\rho C_d A_{ref} v^2 \right] - \mu g \cos(\delta\beta(t)) - g \sin(\delta\beta(t)) \quad (17)$$

This added contribution can be effectively linearized to take the following form:

$$\dot{v} = \frac{1 - \epsilon_m}{m} \left[ F(t) - \frac{1}{2}\rho C_d A_{ref} v^2 \right] - \mu g \cos(\delta\beta(t)) - g \sin(\delta\beta(t)) \quad (18)$$

The original longitudinal model in (9) can be subtracted from (18) to give the following expression for our new  $\delta\dot{v}$ :

$$\delta\dot{v}(t) = -\frac{\epsilon_m}{m} \left[ (F_0 + \delta F(t)) - \frac{1}{2}C_d \rho A_{ref} (v(t))^2 \right] - \frac{C_d}{m} \rho A_{ref} v(t) \delta v(t) \quad (19)$$

where

$$v(t) = v_0 + \delta v_n(t) \quad (20)$$

$$\dot{v}(t) = \dot{v}_0 + \delta \dot{v}(t) = \delta \dot{v}(t) \quad (21)$$

and  $\delta v_n(t)$  is represented by (15-16) in Section 4.1. An interesting and key note is that, upon dividing through by  $\epsilon_m$ , we obtain a simple time varying parameter 1st order ordinary differential equation which we can solve directly for the sensitivity  $\frac{\delta v(t)}{\epsilon_m}$ :

$$\frac{\delta \dot{v}(t)}{\epsilon_m} = -\frac{1}{m} \left[ (F_0 + \delta F(t)) - \frac{1}{2} C_d \rho A_{ref} (v(t))^2 \right] - \frac{C_d}{m} \rho A_{ref} v(t) \frac{\delta v}{\epsilon_m} \quad (22)$$

where  $v(t)$  is sourced from (20). We can also divide by an additional constant  $m$  to obtain proper, non normalized, sensitivity for use in our Fisher analysis. However, the non normalized Fisher information matrix is frequently ill conditioned, so normalization is a valuable tool that improves the numerical tractability of the overall analysis.

We use the MATLAB symbolic algebra toolbox to analytically solve this ODE for  $\frac{\delta v(t)}{\epsilon_m}$ . For the purpose of brevity we omit the final, lengthy, analytic expression for  $\frac{\delta v(t)}{\epsilon_m}$ .

#### 4.2.2. Sensitivity of Velocity with Respect to Drag Coefficient Parameter

Obtaining an expression for the sensitivity of velocity with respect to the vehicle drag coefficient parameter  $C_d$  can be accomplished through a similar procedure as that outlined in the previous subsection 4.2.1. First, for our longitudinal model in (9), we add a percent perturbation to the parameter  $C_d$ :

$$\dot{v}(t) = \frac{1}{m} \left[ F(t) - \frac{1}{2} \rho C_d (1 + \epsilon_{C_d}) A_{ref} (v(t))^2 \right] - \mu g \cos(\delta \beta(t)) - g \sin(\delta \beta(t)) \quad (23)$$

Subtracting (9) from this equation gives us our next formulation for our new  $\delta \dot{v}$ :

$$\delta \dot{v}(t) = -\frac{\epsilon_{C_d}}{2m} C_d \rho A_{ref} (v(t))^2 - \frac{C_d}{m} \rho A_{ref} v(t) \delta v \quad (24)$$

where  $v(t)$  similarly takes the form of (20). Dividing (24) through by  $\epsilon_{C_d}$  conveniently yields an ODE format with respect to the sensitivity variable  $\frac{\delta v(t)}{\epsilon_{C_d}}$ :

$$\frac{\delta \dot{v}(t)}{\epsilon_{C_d}} = -\frac{1}{2m} C_d \rho A_{ref} (v(t))^2 - \frac{C_d}{m} \rho A_{ref} v(t) \frac{\delta v(t)}{\epsilon_{C_d}} \quad (25)$$

Substituting (20) and solving via MATLAB's symbolic engine yields an analytic expression for the sensitivity  $\frac{\delta v(t)}{\epsilon_{C_d}}$ .

#### 4.2.3. Sensitivity of Velocity with Respect to Rolling Resistance Parameter

Obtaining an expression for the sensitivity of velocity with respect to the vehicle rolling resistance coefficient parameter  $\mu$  can be accomplished through a likewise similar procedure. First, for our longitudinal model in (9), we add a percent perturbation to the

parameter  $\mu$ :

$$\dot{v}(t) = \frac{1}{m} [F(t) - \frac{1}{2} \rho C_d A_{ref} (v(t))^2] - \mu(1 + \epsilon_\mu) g \cos(\delta\beta(t)) - g \sin(\delta\beta(t)) \quad (26)$$

Subtracting (9) from this equation gives us our next formulation for our new  $\delta\dot{v}(t)$ :

$$\delta\dot{v}(t) = -\epsilon_\mu \mu g \cos(\beta(t)) - \frac{C_d}{m} \rho A_{ref} v(t) \frac{\delta v(t)}{\epsilon_\mu} \quad (27)$$

where we substitute the expression in (20) for  $v(t)$ , as was the case in our prior derivations. Dividing (27) through by  $\epsilon_\mu$  conveniently yields an ODE format with respect to the sensitivity  $\frac{\delta v(t)}{\epsilon_\mu}$ :

$$\frac{\delta\dot{v}(t)}{\epsilon_\mu} = -\mu g \cos(\beta(t)) - \frac{C_d}{m} \rho A_{ref} v(t) \frac{\delta v(t)}{\epsilon_\mu} \quad (28)$$

In this case, MATLAB's symbolic engine yields an analytic sensitivity expression which is short enough to include in this subsection:

$$\frac{\delta v(t)}{\epsilon_\mu} = e^{\frac{\int_0^t (C_d A_{ref} \rho (m v_0 + \sigma(\tau))) d\tau}{m^2}} \int_0^t \left[ -g \mu \cos(\delta\beta(t)) e^{\frac{\int_0^\tau (C_d A_{ref} \rho (m v_0 + \sigma(u))) du}{m^2}} \right] d\tau \quad (29)$$

$$\sigma(u) = e^{\frac{C_d A_{ref} \rho v_0 u}{m}} \int_0^u \left[ e^{\frac{C_d A_{ref} \rho v_0 w}{m}} (\delta F(w) - mg(\sin(\delta\beta(w)) - \mu + \mu \cos(\delta\beta(w)))) \right] dw \quad (30)$$

#### 4.3. Simulation and Experimental Validation of Sensitivity Expressions

To validate our analytic sensitivity expressions, we utilize both a simulation study and an experimental analysis. First, in our simulation study, we compute a representative driving segment with sufficient excitation. Then, we simulate longitudinal driving along that segment subject to the same longitudinal model parameterization given in [9] corresponding to a Volvo VNL300 heavy-duty vehicle, namely  $m = 8875$  kg,  $C_d = 0.49$ , and  $\mu = 0.0056528$ . Using the data from this simulated driving, we compute the parameteric sensitivity signals using expressions given in Section 4.2 of this paper and those we obtain through (5). For our analytic expressions, we take the operating points as (1) the average measured velocity and (2) the average measured wheel force. Figure 1 demonstrates this comparison for 20 minutes of simulated driving. The sensitivities plotted in Figure 1 are not normalized. As we can see, even with a relatively large range of velocities the requisite approximations we make in our analytic derivations end up having little effect on the accuracy of our final results. Furthermore, the Cramér-Rao bounds we obtain from this simulation using numerical and analytic sensitivities are in strong agreement. Table 2 lists the estimation error bounds from both numerical and analytic sensitivities.

For our experimental study, we use data from an instrumented heavy-duty vehicle driving on-road to validate our analytic sensitivity expressions. The experimental vehicle is instrumented with a final-drive torque sensor, GPS, and a CAN interface which logs data through a Simulink real-time machine. The precise details of this experimental setup can be referenced in [9]. This setup allows us to record values of wheel torque,

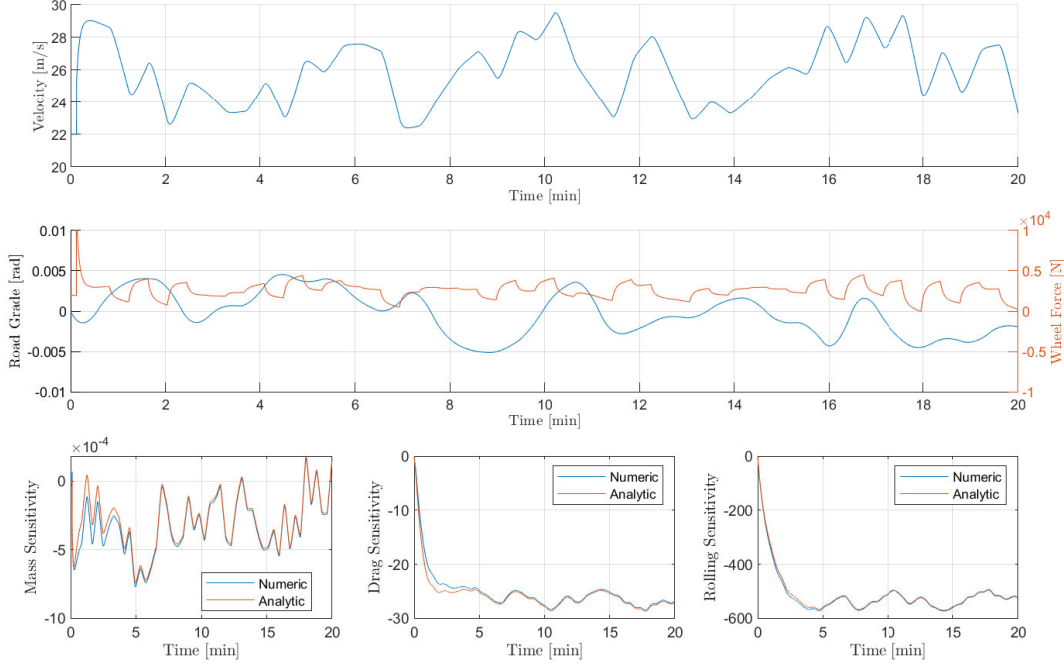


**Figure 1.** Simulated validation of analytic sensitivity derivation

**Table 2.** Cramér-Rao Bounds from Simulated and Experimental Validation of Sensitivity

Estimation Error	Numerical (sim)	Analytic (sim)	Numerical (exp)	Analytic (exp)
Mass $m$ [kg]	47.30	48.00	26.91	28.89
Drag Coefficient $C_d$ [-]	0.0043	0.0039	0.0108	0.0091
Rolling Resistance $\mu$ [-]	0.00022	0.00020	0.00086	0.00078

road grade, velocity and acceleration, braking indicator, and other useful signals. To conduct our experimental comparison, we cut the data using the braking indicator to avoid unmodeled braking dynamics. Then, we compute the sensitivities of the vehicle velocity with respect to each nominal parameter value both numerically and using our analytic expressions. Figure 2 demonstrates the results of this comparison. Overall, we observe strong agreement between numeric and analytic sensitivity signals for highway driving. Upon computing the Fisher information matrices for both the analytic and numeric cases, our resulting Cramér-Rao estimation error lower bounds also agree. Table 2 shows the Cramér-Rao bounds obtained from the above data sample.

#### 4.4. Interpretation

Unfortunately, these analytic sensitivity equations are largely too complex to qualitatively interpret. We can, however, identify some influences of terrain on the output sensitivity. Generally speaking, based on the small angle approximation  $\cos(\theta) \approx 1 - \frac{\theta^2}{2}$ , several of the sensitivities depend roughly on the integral of road grade squared.

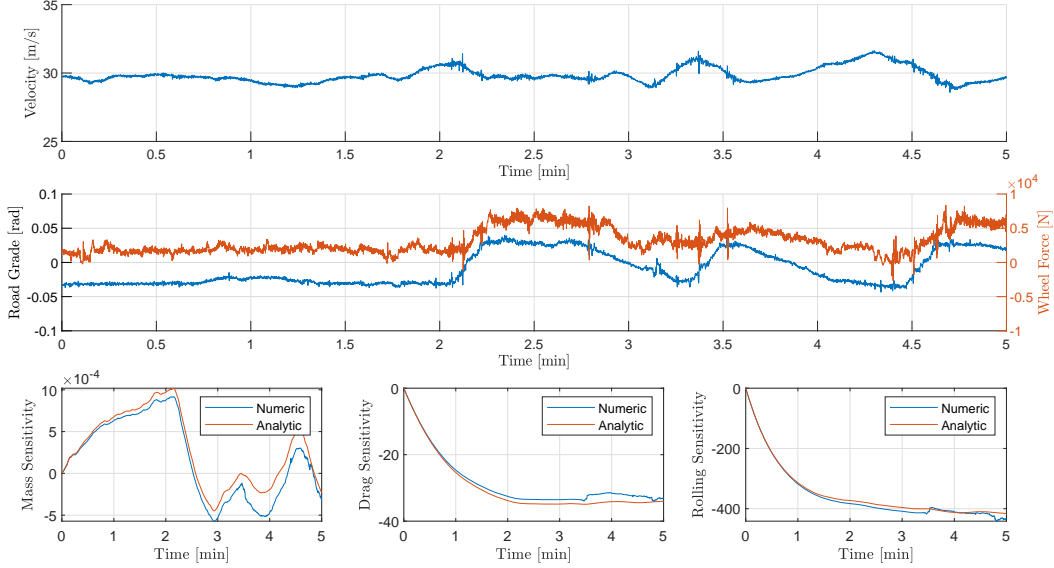


**Figure 2.** Experimental validation of analytic sensitivity derivation

## 5. Fisher Information Analysis

This section details several simulation studies which explore how the terrain variability of a sample of data is directly related to the identifiability of longitudinal chassis parameters estimated from that data. This relationship shares relevance for on-road experimental design, and potentially for applications where online vehicle parameter estimation serves an important purpose. This paper quantifies parameter identifiability through relevant quantities pertaining to the Fisher information matrix, including its normalized determinant and trace (obtained using percent/normalized sensitivities) in addition to the estimation error bounds obtained from the covariance matrix. Using the determinant or trace of Fisher information is consistent with D and A optimal design methodologies, respectively [19]. These metrics are related to a quantification of terrain variability observed in the data, specifically through the following mean-square terrain variability metric:

$$\xi = \frac{\sum_{i=1}^N \beta_{i;road}^2}{N} \quad (31)$$

where  $N$  is the total number of data points in the overall drive-cycle. This metric has units radians<sup>2</sup>. This representation of terrain variability aligns with the insights we are able to glean from our analytic sensitivity derivations.

This section includes three primary types of Monte Carlo simulation studies under which we evaluate longitudinal chassis parameter identifiability. They cover conditions which control for effects from propulsion force, speed trajectory, and mixed conditions..

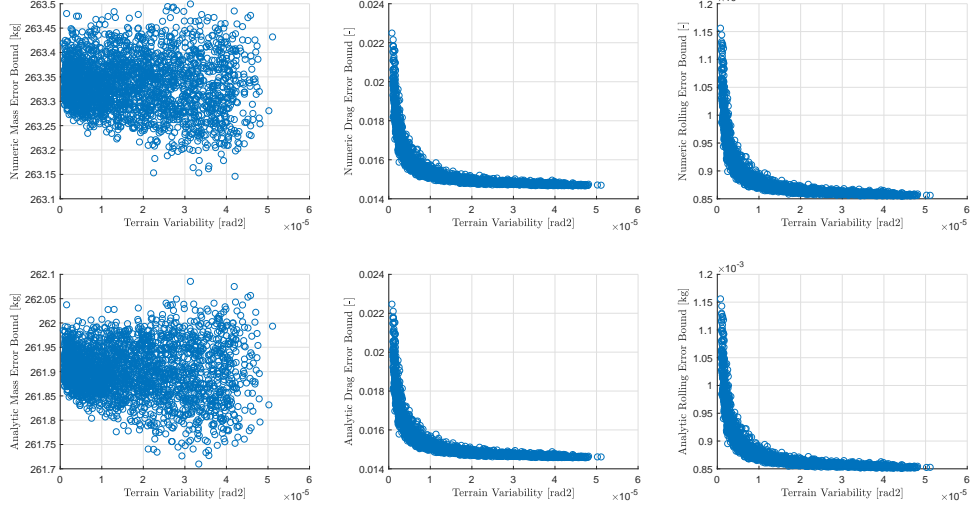


**Figure 3.** Cramér-Rao error bounds for our consistent force simulation study

### 5.1. Consistent Force Simulations

Our first type of Monte-Carlo simulation study is characterized by each experiment sharing the exact same propulsion force trajectory. Specifically, we first generate 2500 random road terrain profiles. For each road terrain segment, we vary the maximum allowed road grade magnitude between 0.002 and 0.014 radians. We accomplish this by generating piecewise-linear road grade signals and then subjecting them to a low-pass filter with cutoff frequency  $\omega_c = 3 \frac{\text{rad}}{\text{s}}$ . One example of this procedure is given by the terrain profile shown in Figure 1. For the vehicle mass (8875 kg), we compute the propulsion force required for the vehicle to travel at  $25 \frac{\text{m}}{\text{s}}$ , and then apply the force perturbation  $\delta F(t) = 600 \sin(0.2t)$  to ensure persistence of excitation. We then simulate driving on each road segment for 4000 seconds and compute the Fisher information matrix around a nominal parameterization using both numerical and analytic methods. Finally, we compare (1) Cramér-Rao estimation error bounds and (2) properties of the Fisher information matrix (including determinant and trace) between the numeric and analytic methods indexed by the mean-square terrain variability of each road segment. We apply this simulation study to demonstrate the on average trend between road terrain variability and vehicle chassis parameter identifiability. Figure 3 shows a comparison of Cramér-Rao bounds for our consistent force simulation study.

As shown in Figure 3, the mean-square road terrain variability is strongly correlated with vehicle chassis parameter identifiability. This is especially true for the  $C_d$  and  $\mu$  parameters. An important note is that, compared to the past results we present in [9], this relationship possesses variability *around* a monotonic trend. The robust design of our updated simulation study methodology reveals this relationship.

Figure 4 shows the determinant and trace of the Fisher information matrices for this same batch of simulations, obtained using normalized output sensitivities. As is the case for A and D optimal experimental design, maximizing the trace and determinant, respectively, of the Fisher information matrix is consistent with maximizing parameter identifiability. From this figure it is therefore clear that on average, driving on roads with higher mean-square terrain variability yields better overall chassis parameter

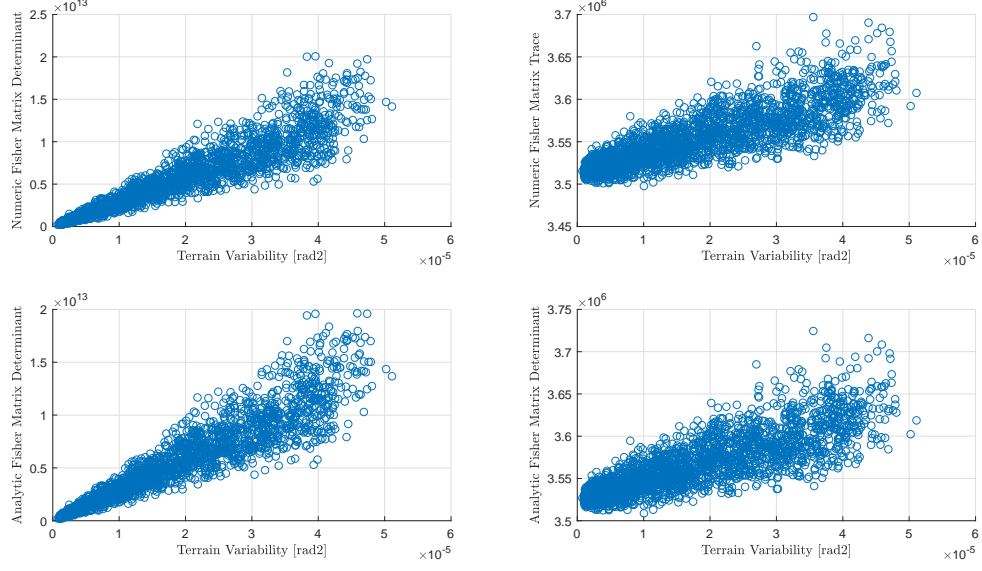


**Figure 4.** Fisher information matrix properties for consistent force simulations

identifiability. The fact that this relationship is maintained on average could be due to a host of underlying factors, including the range and excitation provided by the resulting velocity signal of the experiment.

### 5.2. Consistent Speed Simulation Studies

This paper also presents a series of consistent speed simulation studies to explore the relationship between terrain variability and vehicle chassis parameter identifiability. Now, instead of applying a sinusoidally varying propulsion force, we solve the longitudinal model backwards for the propulsion force signal which allows the vehicle to maintain a velocity signal which we define a priori. The key difference between these simulations and those detailed in the previous section is that here, we simulate a vehicle driving the same velocity profile across each unique road grade segment. We accomplish this through the following method. First, we generate a random velocity signal consistent with our approach to generating road grade signals. Figure 5 shows this velocity signal.

Then, using the road grade signals and differentiated velocity signal, we calculate the propulsion force which yields the desired velocity profile for the given terrain profile. This calculation is simple, as we can use the longitudinal model directly:

$$F(t) = m\dot{v}(t) + \frac{1}{2}C_d\rho A_{ref}(v(t))^2 + \mu mg \cos(\beta(t)) + mg \sin(\beta(t)) \quad (32)$$

In this simulation study, our objective is to explore the relationship between terrain variability and chassis parameter identifiability when we control for a different signal, namely velocity. Figure 5 shows the constant velocity signal. Figure 6 shows the Cramér-Rao error bounds from this analysis for the same 2500 random road terrain profiles. Here, the Cramér-Rao estimation error bounds adopt different trends.

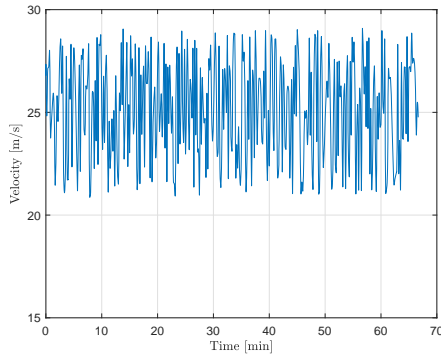


**Figure 5.** Consistent velocity signal

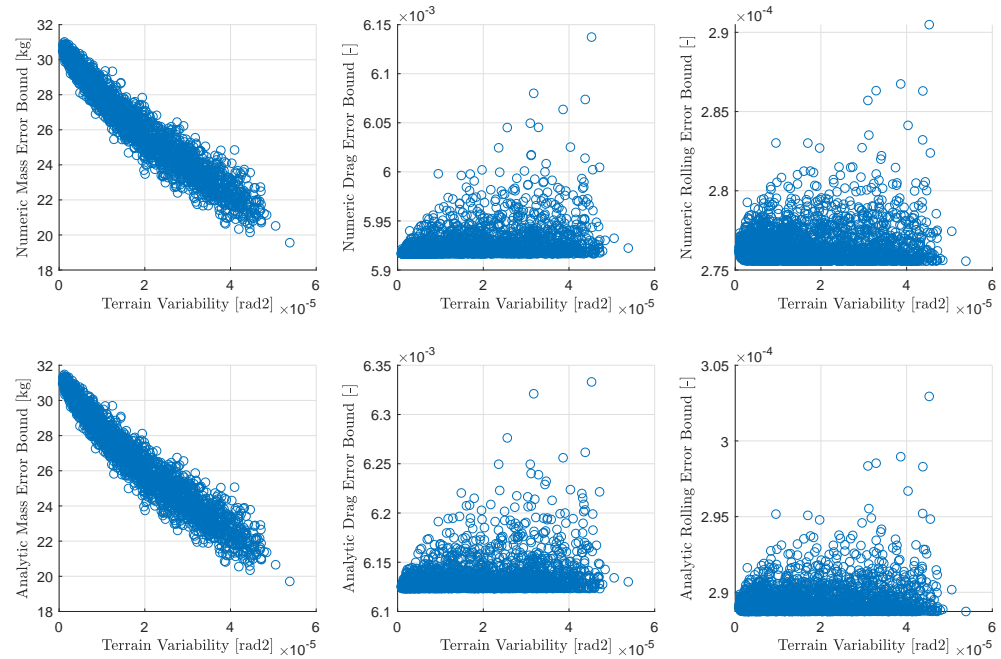


**Figure 6.** Cramér-Rao error bounds for our consistent speed simulation study

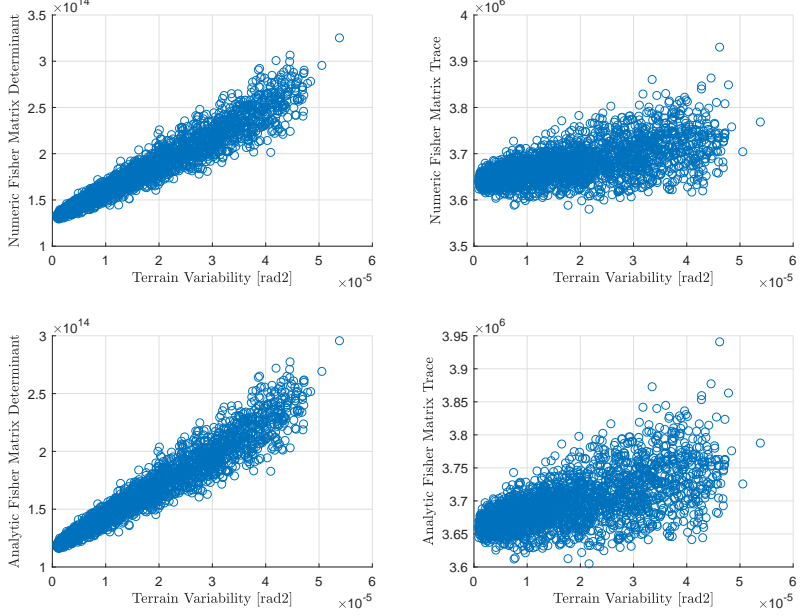


**Figure 7.** Fisher matrix properties for our consistent speed simulation study

However, the trends observed in the Fisher information determinant and trace shown in Figure 7 demonstrate on-average improvements in chassis parameter identifiability from roads with higher overall terrain variability. In this case, most of the individual improvement in parameter identifiability is seen by the mass parameter, which sees significantly better estimation error improvement compared to our consistent force simulations. This is likely due to the fact that, as the terrain variability increases, the overall excitation from the propulsion force becomes much greater in order for the vehicle to maintain the same speed profile. In the original nonlinear ODE of the longitudinal dynamics, the mass dependent component is predominantly sourced from the propulsion force term, so this relationship makes intuitive sense. The other parameters see very limited difference in overall identifiability. While the trend ostensibly appears to be that identifiability generally worsens for  $C_d$  and  $\mu$  as mean-square terrain variability of the experiment increases, the total change in the upper bound is minimal compared to the nominal parameter value. Furthermore, most of the estimation error bounds for  $C_d$  and  $\mu$  are centered near what appear to be strong lower bounds which are constant in mean-square terrain variability. The presence of these strong lower bounds is also an interesting feature to note from this simulation study.

### 5.3. Mixed Condition Simulation Study

Finally, to complement the results for this paper's previous sections, we present a simulation study which explores the relationship between terrain variability and chassis parameter identifiability under mixed driving conditions. Our mixed condition simulations follow the procedure outlined for a consistent speed simulation identically, except the force we uniquely calculate to maintain a predefined constant velocity trajectory is multiplied by a factor of 0.85. This is our representation of actual on-road driving con-

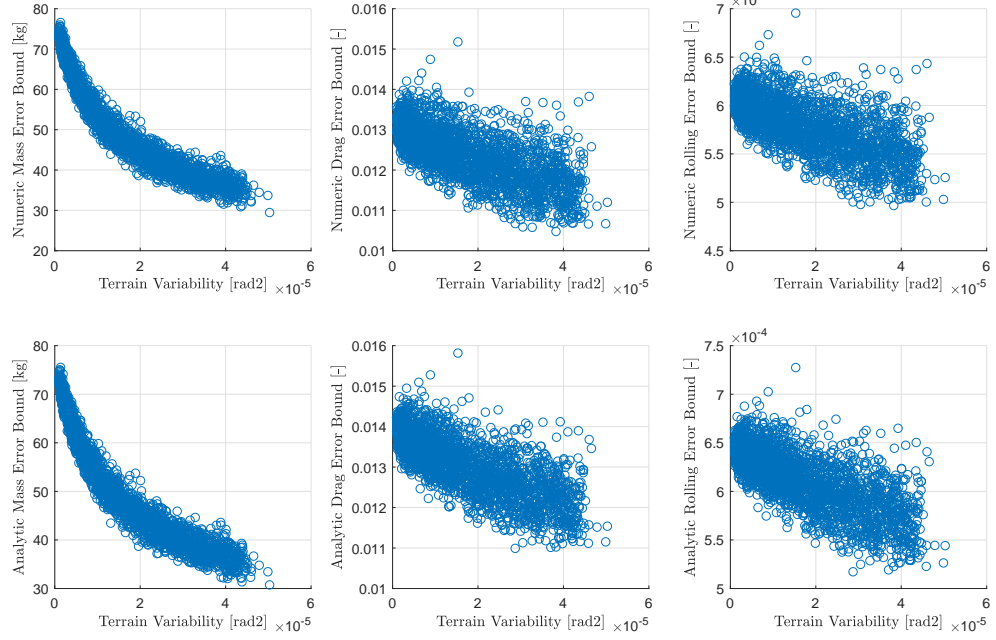


**Figure 8.** Cramér-Rao error bounds for mixed simulation study

ditions, where the propulsion force dictated by the driver in small part depends on the road grade profile. Thus, the vehicle in this type of simulation will slow down slightly when traveling uphill and will speed up slightly when driving downhill. This design can't control the contributions of propulsion force and velocity range completely, but it presents an interesting opportunity to study the impact both variables have for drive cycles with progressively hillier terrain. Figures 8 and 9 present our results from this analysis.

## 6. Conclusion

This paper presents two key contributions. These include (i) simple analytic derivations of the Fisher information matrix associated with estimating vehicle mass, drag, and rolling resistance coefficient parameters from a longitudinal vehicle dynamics model, and (ii) a series of Monte Carlo simulation studies which illustrate the relationships between terrain variability and longitudinal chassis parameter identifiability.

Our objective in obtaining analytic velocity sensitivity expressions is to glean insights about which chassis parameters and signals imposed the greatest impact on chassis parameter identifiability. Despite several necessary approximations, these expressions are simply too cumbersome to accommodate this objective. However, our analytic expressions possess an impressive degree of accuracy relative to sensitivity signals obtained numerically. We demonstrate this finding using simulations and experimental validation. We observe the greatest accuracy when a limited range of velocities are present in the drive cycle. Additionally, our results indicate the analytic expressions can compute estimation error bounds far faster than numeric approximations which require the longitudinal dynamics model to be solved numerically as a

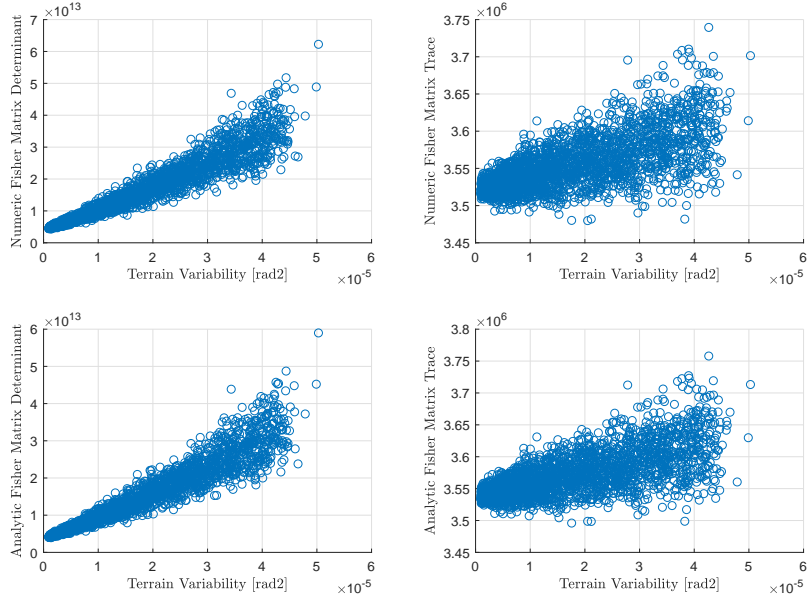


**Figure 9.** Fisher matrix properties for mixed simulation study

nonlinear ordinary differential equation. Perhaps this computational speed will provide the greatest utility if such analytic expressions are incorporated into real-time longitudinal chassis parameter estimation applications.

This paper also illustrates the following for randomized simulations of longitudinal driving over numerous drive cycles with varying road grade profiles. When propulsion force is kept constant across different drive cycles, parameter identifiability improves on average for drive cycles associated with higher terrain variability, with the greatest improvements seen by the estimation error bounds for the drag and rolling resistance parameters. When the speed profile is kept constant for different drive cycles through perfect feedback control of the propulsion force signal, parameter identifiability as quantified by the determinant and trace of the normalized Fisher information matrices improves. This manifests with strong improvements in mass estimation error with greater mean-square terrain variability, and generally inconclusive trends observed in  $C_d$  and  $\mu$  estimation error bounds. Under mixed conditions, where the propulsion force required to maintain a specified velocity trajectory is computed and slightly scaled down, parameter identifiability improves uniformly on average for all three relevant longitudinal chassis parameters.

These results imply several meaningful insights which have direct applications to burgeoning research in automotive controls. Principal among these insights is that, on average, drive cycles characterized by higher degrees of terrain variability generally allow longitudinal chassis parameters to be estimated more accurately. The first application of this insight pertains directly to the design of on-road experiments for longitudinal chassis parameter identifiability. Choosing routes for such experiments which possess the greatest degree of terrain variability could not only improve the accuracy of parameter estimates obtained from the experiment, but could also enable researchers to avoid unnecessarily precise and costly instrumentation. Perhaps more significant than the application to experimental design is the relevance of this paper's

results to connected and automated vehicle (CAV) systems research. Much of this research relies on a priori knowledge of relevant vehicle parameters, including vehicle mass, drag, and rolling resistance coefficients. For actual implementation of CAV system optimization, these parameters may in fact need to be estimated in real time with online parameter estimation algorithms, and such algorithms will need to interface with system-wide optimization. The effectiveness of CAV optimization algorithms will likely depend on the accuracy of these parameter estimates, and as a result choosing and weighting data from segments of road characterized by high terrain variability may improve the function of such algorithms.

### **Acknowledgement**

The authors thank the engineers from Volvo Powertrain North America who assisted with the experimental work utilized in section IV of this paper.

### **Funding**

This work is supported by a National Science Foundation Graduate Research Fellowship, and by NSF award #CMMI-1538300 and ARPA-E award #DE-AR0000801.

## References

- [1] Papelis, Y., Brown, T., Watson, G., Holz, D., and Pan, D., 2004, Study of ESC Assisted Driver Performance Using a Driving Simulator, Document ID: N04-033- PR, Published by University of Iowa, National Advanced Driving Simulator.
- [2] Zabat, M., Farascaroli, S., Browand, F., Nestlerode, M., and Baez, J. (1994), Drag Measurements on a Platoon of Vehicles. Report from Institute of Transportation Studies at UC Berkeley, California PATH program, 1994.
- [3] He, C., Ge, J., and Orosz, G. (2018), Data-based fuel-economy optimization of connected automated trucks in traffic. Proceedings of the 2018 American Control Conference. Milwaukee, WI USA, June 2018.
- [4] Xu, C., Geyer, S., and Fathy, H. K. (2019), Formulation and Comparison of Two Real-Time Predictive Gear Shift Algorithms for Connected/Automated Heavy-Duty Vehicles. IEEE Transactions on Vehicular Technology, vol 68 number 8, pp. 7498-7510.
- [5] Bae, H. S., Ryu, J. and Gerdies, J. C. (2001). Road Grade and Vehicle Parameter Estimation for Longitudinal Control Using GPS. 2001 IEEE Intelligent Transportation Systems Conference. Oakland, CA: 2001 IEEE Intelligent Transportation Systems Proceedings, pp.166-71.
- [6] Fathy, H. K., Kang, D. and Stein, J. L., (2008). Online vehicle mass estimation using recursive least squares and supervisory data extraction. Proceedings of the 2008 American Control Conference (ACC). Seattle, WA USA, June 2008.
- [7] A. Vahidi, A. Stefanopoulou and H. Peng (2005) Recursive least squares with forgetting for online estimation of vehicle mass and road grade: theory and experiments, Vehicle System Dynamics, 43:1, 31-55, DOI: 10.1080/00423110412331290446
- [8] Rhode, S. and Gauthier, F. (2013). Online estimation of vehicle driving resistance parameters with recursive least squares and recursive total least squares. Proceedings of the 2013 IEEE Intelligent Vehicles Symposium (IV). Gold Coast, Australia, June 2013.
- [9] Kandel, A. I., Wahba, M., Geyer, S. and Fathy, H. K. (2018). Impact of terrain variability on chassis parameter identifiability for a heavy-duty vehicle. Proceedings of the 2018 European Control Conference (ECC). Limassol, Cyprus, June 2018.
- [10] Rajamani, R., and Hedrick, J. K., 1995, "Adaptive Observers for Active Automotive Suspensions: Theory and Experiment", IEEE Transactions on Control System Technology, 3(1), pp. 86-93.
- [11] Pence, B., Fathy, H. K. and Stein, J. L. (2009). Sprung mass estimation for off-road vehicles via base-excitation suspension dynamics and recursive least squares. Proceedings of the 2009 American Control Conference. St. Louis: IEEE, pp.5043- 5048
- [12] Reina, G., Paiano, M., and Blanco-Claraco, J., Vehicle parameter estimation using a model-based estimator, Mechanical Systems and Signal Processing, Volume 87, Part B, 2017, Pages 227-241, ISSN 0888-3270, <https://doi.org/10.1016/j.ymssp.2016.06.038>.
- [13] Bellman, R., and Astrom, K. J. (1970). On Structural Identifiability. Mathematical Biosciences, 7, 329-339. [https://doi.org/10.1016/0025-5564\(70\)90132-X](https://doi.org/10.1016/0025-5564(70)90132-X)
- [14] SAE International (2008). SAE standard J2263: Road Load Measurement Using Onboard Anemometry and Coastdown Techniques. Light Duty Vehicle Performance and Economy Measure Committee. SAE International, pp.1-12
- [15] Muller, T., Ferris, J., Detweiler, Z. and Smith, H. (2009). Identifying vehicle model parameters using measured terrain excitations. SAE Technical Papers
- [16] Rajamani, R., Vehicle Dynamics and Control, 2nd ed. Springer US, 2012, vol. 14.
- [17] Norton, J. P., An Introduction to Identification, 1st ed. Dover, 1986.
- [18] Thomas, J. and Cover, T., Elements of Information Theory, 2nd ed. Wiley, 1991.
- [19] Goss, P. and Jones, B., Optimal Design of Experiments: A Case Study Approach, 1st ed. Wiley, 2011.